

Mechanism and experimental study on the fruit detachment of Chinese wolfberry through reciprocating vibration

Song Mei^{1,2}, Jinpeng Wang³, Zhiyu Song², Dunbing Tang^{1*}, Cheng Shen²

(1. College of Mechanical and Electrical Engineering, Nanjing University of Aeronautics and Astronautics, Nanjing 210016, China;

2. Nanjing Research Institute for Agricultural Mechanization, Ministry of Agriculture and Rural Affairs, Nanjing 210014, China;

3. Nanjing Forestry University, Nanjing 210037, China)

Abstract: In order to realize the efficient and high-quality mechanical picking for Chinese wolfberry, firstly, the forced reciprocating vibration picking principle of the Chinese wolfberry branch was studied, and the mechanical model of vibration picking was established based on the simplified cantilever model, and the response analysis and solution of all positions for the branch were carried out. At the same time, the critical mechanical model of fruit detachment under the condition of fruit hanging on branches was established, and the theoretical values of inertia force for each component of the branch were obtained. Secondly, through actual measurement and finite element modeling, the natural frequency and forced vibration response simulation for each component of the branch of Chinese wolfberry terminal branch model were both studied, and the relationship between single-point periodic excitation force and high-quality fruit shedding parameters was obtained. Thirdly, according to the conclusion of the picking model, a test bench with many groups of adjustable parameters was built. Finally, the last branch of fruit-hanging Chinese wolf berry for Ningqi No.1 was taken as the experimental object, a four-level orthogonal experiment was designed with three factors: frequency, amplitude and entrance angle. Meanwhile, the net picking rate, damage rate and false picking rate were taken as the evaluating indicators, referring to the comprehensive scores of the three factors. It was concluded that the primary and secondary relations of factors affecting the picking effect are frequency, amplitude and entrance angle, and the best operation parameters are frequency of 20 Hz, amplitude of 15 mm, and entrance angle of 45°, then, a hand-held vibration picker with setting parameters was trial-produced, and the optimal parameter combination was verified in the Chinese wolfberry planting base of the National Chinese wolfberry Engineering and Technology Research Center. The results showed that the net picking rate of ripe Chinese wolfberry was 96.13%, the damage rate of fruit was 1.13%, and the false picking rate was 3.23%, mechanized picking efficiency was 30.28 kg/h, which is 6.65 times that of manual picking. The experimental results are consistent with the simulation results. The research results can provide an important basis for the creation and operation standards of large-scale Chinese wolfberry vibration harvesting equipment.

Keywords: Chinese wolfberry branches, reciprocating vibration, inertial force, orthogonal experiment

DOI: [10.25165/j.ijabe.20241702.8482](https://doi.org/10.25165/j.ijabe.20241702.8482)

Citation: Mei S, Wang J P, Song Z Y, Tang D B, Shen C. Mechanism and experimental study on the fruit detachment of Chinese wolfberry through reciprocating vibration. *Int J Agric & Biol Eng*, 2024; 17(2): 47–58.

1 Introduction

Chinese wolfberry, primarily found in China and sparsely distributed in Korea, Japan, and Europe, is deemed a characteristic cash crop in China's agricultural landscape. Belonging to the berry category, Chinese wolfberry is susceptible to damage, but it has high medicinal and nutritional values because it is rich in polysaccharides, amino acids, vitamins, and trace elements needed by the human body^[1]. The primary cultivation regions encompass Ningxia, Inner Mongolia, Gansu, and Xinjiang, collectively

accounting for an expansive planting area exceeding 3 million acres^[2,3]. However, the growth of the Chinese wolfberry industry underscores the escalating prominence of challenges that impede its progress, including issues related to timeliness of harvesting, labor scarcity, and elevated production costs, which urgently need these limitations to be addressed through mechanization to improve labor efficiency. The present manual harvest efficiency for Chinese wolfberry stands at a mere 3-5 kg/h, with manual harvesting expenses accounting for over 40% of the overall production costs. With the rising cost of harvesting, the harvesting problem has become a bottleneck restricting the sustainable development of the goji berry industry^[4]. Notably, a conspicuous absence persists in the market concerning a fully developed mechanized harvesting apparatus tailored for Chinese wolfberry. While various berry harvesting techniques such as vibration, combing, shearing, and pneumatic methods are extant globally, Chinese wolfberry's unique attributes are only partially compatible^[5]. The distinctive growth pattern characterized by "continuous flowering and fruiting", compounded by the intricate physical and mechanical properties of the Chinese wolfberry and its branches, underscores the endeavor's complexity. With fruits ripening in stages, boasting delicate and thin skins, and further complicated by variant physical and mechanical characteristics across diverse varieties, the pursuit of mechanized

Received date: 2022-12-08 **Accepted date:** 2024-01-08

Biographies: Song Mei, Associate Professor, research interest: agricultural mechanization engineering for fruits, Email: meisong@caas.cn; Jinpeng Wang, Associate Professor, research interest: agricultural engineering, Email: 2942518392@qq.com; Zhiyu Song, Associate Professor, research interest: agricultural mechanization engineering, Email: songzhiyu@caas.cn; Cheng Shen, research assistant, research interest: agricultural engineering, Email: shencheng@caas.cn.

***Corresponding author:** Dunbing Tang, Professor, research interest: intelligent agriculture. College of Mechanical and Electrical Engineering, Nanjing University of Aeronautics and Astronautics, No.29, Yudao Street, Qinhuai District, Nanjing 210016, China. Tel: +86-13776639985, Email: d.tang@nuaa.edu.cn.

harvesting characterized by high precision (high fruit shedding rate, minimal damage rate, and negligible false picking rate) encounters significant technical bottlenecks. Unfortunately, these limitations hinder the optimization of the Chinese wolfberry industry's structural composition, the augmentation of farmers' income, and the revitalization and development of rural regions.

In recent years, the imperative for Chinese wolfberry industry development to be encouraged has necessitated the advent of Chinese wolfberry harvesting machinery. Support of paramount significance is lent by both the Ministry of Science and Technology and the Science and Technology Department of the Chinese Wolfberry Province in fostering research regarding the mechanized harvesting technology of Chinese wolfberry. The research encompassing Chinese wolfberry harvesting technology in China can be chiefly categorized into two distinct classifications. The former entails the exploration of a hand-held portable device devised for Chinese wolfberry harvesting, which can be cooperated with manual operation. It is poised to augment operational efficiency over threefold while concurrently mitigating labor intensity^[6,7]. Conversely, the latter classification explores self-propelled continuous harvesting technology for Chinese wolfberry^[8,9]. This mechanized modality of operation demonstrates an efficiency surpassing more than twentyfold that of manual labor, thereby efficaciously tackling the difficulty of Chinese wolfberry industry development. Nonetheless, the latter classification of Chinese wolfberry harvesting equipment tends to manifest certain predicaments, including but not limited to a low net picking rate, significant damage, and a series of erroneous picking instances^[10]. Consequently, the immediate commercial viability of self-propelled Chinese wolfberry continuous harvesting equipment remains elusive.

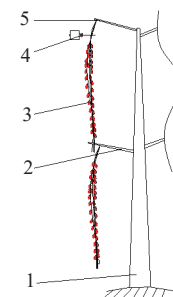
To achieve efficient and high-quality harvesting of Chinese wolfberries during the effective harvesting period, this study focuses on exploring suitable methods that will overcome the technical bottleneck associated with mechanical energy. Comparative experiments show that reciprocating vibration, vibration, and pneumatic harvesting are compatible with developing continuous harvesting technology and equipment for self-propelled Chinese wolfberry harvesting^[11,12]. Of particular note is the reciprocating vibration mode, which demands relatively modest harvesting conditions, exhibits a conspicuous rate of fruit detachment in Chinese wolfberries, and reveals damage causes that necessitate further practical exploration. However, the relationship between damage and fruit abscission rate remains closely intertwined, and researchers have yet to undertake a specific analytical investigation into this connection. Zhang et al.^[13] conducted an initial theoretical and practical analysis of the reciprocating vibration method, yet the intricate interplay between amplitude, frequency, and vibration gap has yet to be comprehensively examined. Xu et al.^[14] devised a comb-brush vibration harvesting device, resulting in satisfactory outcomes. Nonetheless, the requisites for its operation pose elevated demands, rendering it unsuitable for large-scale equipment adaptation. Currently, the theoretical basis for the mechanism design of reciprocating vibration harvesting components with a high fruit-dropping rate is lacking^[15-17], and the mechanism of multi-parameter vibration components interacting with branches is unknown, so it is impossible to develop self-propelled continuous harvesting technology and equipment with reliable technology and good operation effect.

In this study, the reciprocating vibration method was proposed

to explore the mechanism of forced vibration of fruit-hanging branches. First, the principle of forced vibration of fruit-hanging branches of Chinese wolfberry was analyzed, and a simplified cantilever forced vibration picking model was constructed; secondly, the theoretical method of branch system response analysis and solution was established, and the response values of each position can be solved by obtaining the physical quantities of the system itself; thirdly, the motion model of fruit-hanging branches was constructed, and the relationship between the response of branches and the stress of fruits was established, to obtain the decisive operation parameters of the inertia force of fruits; then, the typical fruit-hanging branch model was constructed by finite element method, and the modal harmonious response analysis was made, and the fruit binding force was compared to obtain the rule of operation parameters. In addition, according to the adjustable operation parameters, a multi-parameter adjustable vibration picking test bench was trial-produced; finally, Ningqi No.1 was taken as the test object, and a four-level orthogonal test with three factors, namely, cross vibration entrance angle, frequency and amplitude, was designed. Based on the test indexes of net picking rate, damage rate and false picking rate concerning their comprehensive scores, relevant tests were carried out, and the primary and secondary relations of factors affecting the picking effect from big to small were obtained. The optimal design and operation parameters of the reciprocating vibration device were obtained.

2 Forced vibration picking model of fruit-hanging branches of Chinese wolfberry

The principle of forced vibration of fruit-hanging branches of Chinese wolfberry (collectively referred to as the last branches of Chinese wolfberry) is depicted in Figure 1. The vibrating device exerts an exciting force at a specific position on the upper side of the mature fruit of the Chinese wolfberry branch according to the sine law so that the Chinese wolfberry branch is forced to vibrate along the reciprocating direction, and the specific direction is based on the relative angle between the fork rod at the end of the manual hand-held vibrating device and the branch, at the same time, the components such as mature Chinese wolfberry, immature Chinese wolfberries, olives, flowers and leaves distributed on the branch obtain vibration displacement and acceleration response.



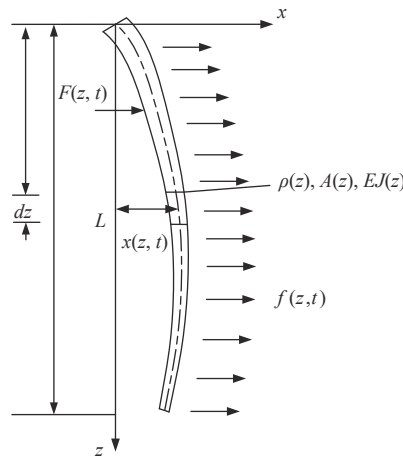
1. Backbone; 2. Lower branching; 3. Terminal branch of Chinese wolfberry; 4. Reciprocating vibration harvester; 5. Upper branching

Figure 1 Schematic diagram of forced vibration picking for Chinese wolfberry

Summer Chinese wolfberry has large yield in China and it is difficult to pick Chinese wolfberry because of its greater stalk strength than autumn fruit. Ningqi No.1 is selected as the research object for summer Chinese wolfberry, and it is divided into five stubbles, which gradually matured from the root to the end of the

last branch. By studying the physical and mechanical characteristics of each component, the characteristics of uniform distribution of each element on the branch according to a specific pitch are obtained. For the convenience of simulation calculation, it is assumed that each component of the fruit-hanging branch is evenly distributed and the spacing is equal. When the vibration device exerts sinusoidal excitation force on the Chinese wolfberry branch, the large-diameter end is fixed, and the other end is free to droop, which can be simplified as a cantilever beam model.

The physical model of terminal branches can be composed of branches and components, from the growth matrix of branches to the cone, with continuous change in mass and decreasing radius of terminal branches. All components are evenly distributed in branches according to a specific pitch. From the overall analysis, all components can be simplified as combining mass and branches. The



distance between each component and branch is equivalent to a rod with negligible mass, and the overall model of fruit-hanging branches with specific taper changes is established.

Define the length of the last branch as L , as shown in Figure 2, the cross-sectional area and the moment of inertia can be established as follows:

$$\begin{cases} A_0 = \frac{\pi d_0^2}{4} \\ J_0 = \frac{\pi d_0^4}{64} \end{cases} \quad (1)$$

where, A_0 is the cross-sectional area at the root of the last branch where $z=0$, m^2 . J_0 is the moment of inertia at the root of the last branch where $z=0$, m^4 . d_0 is the diameter at the root of the last branch where $z=0$, m .

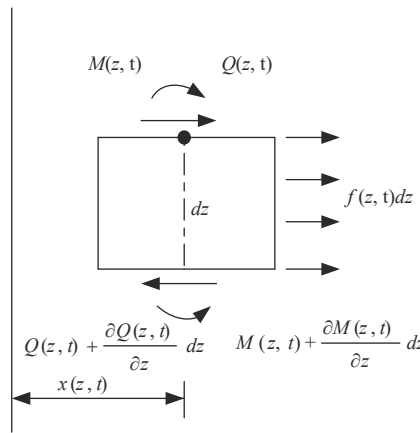


Figure 2 Schematic diagram of the forced vibration picking mechanical model on Chinese wolfberry terminal branches

Call α the coefficient of cross-section change, and the definition equation of α is:

$$\alpha = \frac{d_0 - d_m}{d_0} \quad (2)$$

where, d_m is the diameter at the end $z=L$ of the last branch, m .

From this, the cross-sectional area A_z and moment of inertia $J(z)$ at any section of the last branch are obtained:

$$\begin{cases} A_z = \frac{\pi d_0^2}{4} \left(1 - \alpha \frac{z}{l}\right)^2 \\ J(z) = \frac{\pi d_0^4}{64} \left(1 - \alpha \frac{z}{l}\right)^4 \end{cases} \quad (3)$$

where, A_z is the cross-sectional area at any section of the last branch, m^2 . $J(z)$ is the moment of inertia at any section of the last branch, m^4 .

In order to define the quality attribute of the last branch, it is assumed that the overall density of fruit-bearing branches is ρ , and the relationship between the volume and quality of fruit-bearing branches is obtained:

$$m = \int_0^l \rho A(z) dz \quad (4)$$

where, ρ is the overall density of fruit-bearing branch, kg/m^3 ; m is the mass of the last branch, kg .

As shown in Figure 2, the differential equation of the vibration of the terminal branch is established, and the transverse displacement of the beam is represented by $x(z, t)$, which is a binary function of the section position z and time t . The transverse force per unit length acting on the beam is expressed by $f(z, t)$. System

density $\rho(z)$, cross-sectional area $A(z)$, bending stiffness $EJ(z)$, where E is elastic modulus and $J(z)$ is the moment of inertia, as shown in Figure 2a. Take the mass differential element d_m with z coordinates at any position of the last branch for force analysis, and get the force analysis diagram of the differential element at z coordinate, as shown in Figure 2b, where $Q(z, t)$ represents the shear force and $M(z, t)$ represents the bending moment. According to reference^[18], the forced vibration model of the cantilever beam is obtained as follows:

$$\frac{\partial^2}{\partial z^2} \left[EJ(z) \frac{\partial^2 x(z, t)}{\partial z^2} \right] + \rho(z) A(z) \frac{\partial^2 x(z, t)}{\partial t^2} = f(z, t) \quad (5)$$

Where, E stands for elastic modulus of the Chinese wolfberry branch, MPa .

Let $\varepsilon = 1 - \alpha \frac{z}{l}$, $a' = \frac{2\rho^{\frac{1}{4}} l}{\alpha d_0^{\frac{1}{2}} E^{\frac{1}{4}}}$, $b' = \frac{64l^4}{\pi E d_0^4 \alpha^4}$, then $z=g(\varepsilon)=(1-\varepsilon) \frac{l}{\alpha}$, a' and b' are constants, and bring them into the vibration equation, and simplify the vibration equation with ε and t as independent variables:

$$\frac{\partial^2}{\partial \varepsilon^2} \left[\varepsilon^4 \frac{\partial^2 x(g(\varepsilon), t)}{\partial \varepsilon^2} \right] + a'^4 \varepsilon^2 \frac{\partial^2 x(g(\varepsilon), t)}{\partial t^2} = b' \cdot f(g(\varepsilon), t) \quad (6)$$

$F(\varepsilon, t)=b' \cdot f(g(\varepsilon), t)$, $X(\varepsilon, t)=x(g(\varepsilon), t)$ can be transformed into a new vibration equation:

$$\frac{\partial^2}{\partial \varepsilon^2} \left[\varepsilon^4 \frac{\partial^2 X(\varepsilon, t)}{\partial \varepsilon^2} \right] + a'^4 \varepsilon^2 \frac{\partial^2 X(\varepsilon, t)}{\partial t^2} = F(\varepsilon, t) \quad (7)$$

where, $F(\varepsilon, t)$ is the picking exciting force on Chinese wolfberry

terminal branch, N .

Equation (7) is a simplified vibration equation of the Chinese wolfberry terminal branch. According to higher mathematics, its solution along the X direction consists of a general solution of a homogeneous equation and a special solution of a nonhomogeneous equation. However, in the actual vibration process, the vibration output of the twig may be a general solution of a homogeneous equation $X^T(\varepsilon, t)(F(\varepsilon, t) = 0)$ or a special solution of a nonhomogeneous equation $X^*(\varepsilon, t)(F(\varepsilon, t) \neq 0)$, rather than the superposition of the two:

$$X(\varepsilon, t) = \begin{cases} X^T(\varepsilon, t), F(\varepsilon, t) = 0 \\ X^*(\varepsilon, t), F(\varepsilon, t) \neq 0 \end{cases} \quad (8)$$

According to the above equation, the displacement response of the k -th node of the branch is $X_k(\varepsilon, t)$, and the acceleration response is $X_k''(\varepsilon, t)$ during the forced vibration of the fruit-bearing branch; Then, the picking inertia force of the mature Chinese wolfberry at the k -th node is $F_{1k}(\varepsilon, t) = m_{1k}X_k''(\varepsilon, t)$, the picking inertia force of the immature Chinese wolfberry at the k -th node is $F_{2k}(\varepsilon, t) = m_{2k}X_k''(\varepsilon, t)$, the picking inertia force of the olive at the k -th node is $F_{3k}(\varepsilon, t) = m_{3k}X_k''(\varepsilon, t)$, and the picking inertia force of the flower at the k -th node is $F_{4k}(\varepsilon, t) = m_{4k}X_k''(\varepsilon, t)$, where $m_{1k}, m_{2k}, m_{3k}, m_{4k}$ are the mass of a single mature Chinese wolfberry, immature Chinese wolfberry, olive and flower at the k -th node, respectively.

In the actual vibration process, ripe fruits, immature fruits, olives, flowers and leaves are all subjected to picking inertia force. It will be shaken off when the picking inertia force exceeds the binding force between each component and the handle. Let the binding force between mature Chinese wolfberry, immature Chinese wolfberry, olive, flower and stalk be f_1, f_2, f_3, f_4 respectively. In order to ensure the successful picking of mature Chinese wolfberry, other components do not fall off, the following conditions need to be met:

$$\begin{cases} |F_{1k}(\varepsilon, t)| \geq f_{1\max} \\ |F_{2k}(\varepsilon, t)| \leq f_{2\min} \\ |F_{3k}(\varepsilon, t)| \leq f_{3\min} \\ |F_{4k}(\varepsilon, t)| \leq f_{4\min} \end{cases} \quad (k = 1, 2, \dots, n) \quad (9)$$

3 Response analysis and solution of vibration system of Chinese wolfberry terminal branch

Regarding the special solution $X^*(\varepsilon, t)$ of a non-homogeneous differential equation of a vibration system (such as Equation (7)), the Bessel function is quoted, and the solution method is obtained by using its related properties^[19].

In this research, the vibrating parts force the branches to move back and forth, and the periodic force is applied to the model points of the cantilever beam. The regular modal response of the corresponding non-homogeneous differential equation is as follows:

When $F(\varepsilon, t)$ is the point, the periodic exciting force acts on the end branch $g_j l (g_j \in (0, 1])$ of Chinese wolfberry, and the obtained $F(\varepsilon, t)$ can be expressed as:

$$F(\varepsilon, t) = \begin{cases} F_0 \sin(\omega t), & \varepsilon = 1 - \alpha g_j \\ 0, & \varepsilon \neq 1 - \alpha g_j \end{cases} \quad (10)$$

Then:

$$F_k(\varepsilon, t) = F_0 \sin(\omega t) X_k^*(\varepsilon) \Big|_{\varepsilon=1-\alpha g_j} \quad (11)$$

A certain branch position is selected to give a point a periodic

exciting force, and the vibration output responses (including displacement, speed and acceleration, etc.) of different positions of the branch are obtained by combining the above model and solution method. Then, the inertia force of the mature Chinese wolfberry subjected to vibration picking at each node is:

$$\{F_1(t)\} = \text{diag}(m_{11}, m_{12}, \dots, m_{1r}) X^{*r*}(\varepsilon, t) = \{F_{11}(t), F_{12}(t), \dots, F_{1r}(t)\}^T \quad (12)$$

In the same way, the inertia force of immature Chinese wolfberries, olives and flowers subjected to vibration picking can be obtained:

$$\begin{cases} \{F_2(t)\} = \{F_{21}(t), F_{22}(t), \dots, F_{2r}(t)\}^T \\ \{F_3(t)\} = \{F_{31}(t), F_{32}(t), \dots, F_{3r}(t)\}^T \\ \{F_4(t)\} = \{F_{41}(t), F_{42}(t), \dots, F_{4r}(t)\}^T \end{cases} \quad (13)$$

Equations (12) and (13) obtain the response solutions of each component in each position of the branch. However, from the microscopic analysis, because the handle connecting each component with the branch is flexible, there is a phase difference between the movement of each component and the branch, which directly affects the real inertia force of the fruit. Therefore, this study needs to analyze the fruit-hanging micro-branch in depth.

4 Motion analysis of fruit-hanging micro-branches

The movement form of the fruit on the fruit branch under the excitation is complex, and its possible movement forms can be summarized into six kinds: swinging, shaking, twisting, vertical movement, vertical movement of the fruit handle bending and compound movement^[20]. According to the research, a swing is the primary movement form of Chinese wolfberry fruit under the excitation, so the fruit, the fruit stalk and the branch elements connected with the fruit stalk in the branch can be simplified as a simple pendulum system, including the movement of hanging points. The mechanical analysis model is established in Figure 3.

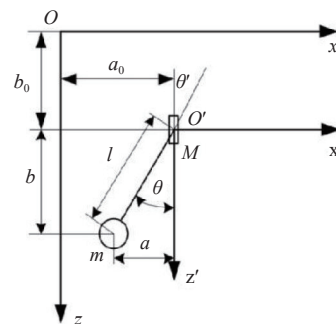


Figure 3 Overall motion model of fruiting micro elements

The kinetic energy and potential energy of the system are:

$$\begin{cases} T = \frac{1}{2} m(\dot{a}^2 + \dot{b}^2) + \frac{1}{2} M(\dot{a}_0^2 + \dot{b}_0^2) \\ V = -(M + m)gX \sin vt \cos \theta - mgl \cos \theta \end{cases} \quad (14)$$

where, T is kinetic energy, J; V is potential energy, J; \dot{a}_0 is velocity of branch infinitesimal in X -axis direction, m/s; \dot{b}_0 is velocity of branch infinitesimal in Z -axis direction, m/s; \dot{a} is velocity of fruit relative to branch element in x axis direction, m/s; \dot{b} is velocity of fruit relative to branch element in z axis direction, m/s; θ is Chinese wolfberry swing angle around the fruit stalk, rad; g is acceleration of gravity, m/s^2 ; X is response amplitude of branches under forced vibration, m; θ is cross vibration entrance angle, rad; v is angular frequency of forced vibration, rad/s; l is fruit stalk length between

branch and Chinese wolfberry, m.

A simple pendulum in xoz coordinate system is:

$$\begin{cases} x = a + a_0 = a_0 \pm l \sin \theta \\ z = b + b_0 = b_0 + l \cos \theta \\ a_0 = X \sin \theta' \sin vt \\ b_0 = X \cos \theta' (1 - \cos vt) \end{cases} \quad (15)$$

Taking θ as the generalized coordinate, we can write the Lagrange function as:

$$L = \frac{1}{2} M (\dot{a}_0^2 + \dot{b}_0^2) + \frac{1}{2} m (\dot{a}_0 + l \dot{\theta} \cos \theta)^2 + \frac{1}{2} m (\dot{b}_0 - l \dot{\theta} \sin \theta)^2 + mgl \cos \theta + (M + m)gX \sin vt \cos \theta' \quad (16)$$

where, $\dot{\theta}$ is Chinese wolfberry swing angle speed around the fruit stalk, rad/s.

The corresponding Lagrange equation is:

$$\frac{d}{dt} \left(\frac{\partial L}{\partial \dot{\theta}} \right) - \frac{\partial L}{\partial \theta} = 0 \quad (17)$$

The differential equation of motion is:

$$\ddot{\theta} + \frac{g}{l} \sin \theta - \frac{\dot{b}_0 \sin \theta - \dot{a}_0 \cos \theta}{l} = 0 \quad (18)$$

Combining Equation (15):

$$\ddot{\theta} + \frac{g}{l} \sin \theta - \frac{X \cos \theta' v^2 \cos vt}{l} \sin \theta - \frac{X \sin \theta' v^2 \sin vt \cos \theta}{l} = 0 \quad (19)$$

$\sin \theta \approx \theta, \cos \theta \approx 1$ can be obtained in the case of micro-small amplitude vibration, and the forced vibration equation can be obtained when the pi of free vibration is $\omega = \sqrt{gl^{-1}}$:

$$\ddot{\theta} + \left(\omega^2 - \frac{X \cos \theta' v^2 \cos vt}{l} \right) \theta - \frac{X \sin \theta' v^2 \sin vt}{l} = 0 \quad (20)$$

Let $\omega_n^2 = \omega^2 - \frac{X \cos \theta' v^2 \cos vt}{l}$, because Equation (20) is a second-order linear non-homogeneous differential equation with constant coefficients, we can learn from the solution method to obtain the full solution as follows:

$$\theta = \frac{X \sin \theta' v^2}{l \left(\omega^2 - \frac{X \cos \theta' v^2 \cos vt}{l} - v^2 \right)} \left(\sin vt - \frac{v}{\omega} \sin \omega t \right) \quad (21)$$

In the process of vibration picking, the fruit is subjected to the normal component of inertia force along the fruit stalk and the tangential component perpendicular to the fruit stalk. The normal component forces the fruit stalk to be axially pulled, and the tangential component forces the fruit to generate a moment at the joint between the fruit stalk and the branches, which causes the fruit to bend between the fruit stalks. In this study, it is considered that the separation of Chinese wolfberry is mainly caused by the pulling force along the fruit stalk, ignoring the tangential force:

$$\begin{cases} F_n = ma_n = ml\ddot{\theta} \\ \dot{\theta} = \frac{X \sin \theta' v^3}{l \left(\omega^2 - \frac{X \cos \theta' v^2 \cos vt}{l} - v^2 \right)} (\cos vt - \cos \omega t) - \frac{X^2 \sin 2\theta' v^5 \sin vt}{2l^2 \left(\omega^2 - \frac{X \cos \theta' v^2 \cos vt}{l} - v^2 \right)^2} \left(\sin vt - \frac{v}{\omega} \sin \omega t \right) \end{cases} \quad (22)$$

where, a_n is normal acceleration of fruit, m/s^2 ; F_n is inertia force of fruit peeling, N.

Since the exciting force of the vibration device on Chinese

wolfberry terminal branch is continuous, if only the forced vibration frequency is considered, Equation (22) can be converted as follows:

$$\begin{cases} \dot{\theta} = -\frac{X \sin \theta' v}{l + X \cos \theta' \cos vt} \cos vt - \frac{X^2 \sin 2\theta' v^3 (\sin vt)^2}{2(X \cos \theta' \cos vt + l)^2} \\ F_n = ml \left(\frac{X \sin \theta' v}{l + X \cos \theta' \cos vt} \cos vt + \frac{X^2 \sin 2\theta' v^3 (\sin vt)^2}{2(X \cos \theta' \cos vt + l)^2} \right)^2 \end{cases} \quad (23)$$

Therefore, the fruit can be separated by ensuring that the normal inertial force of the fruit stalk is greater than the binding force of the fruit stalk, $F_n > F_T$. The main factors leading to the separation of Chinese wolfberry are the amplitude, frequency and forced vibration direction of the micro-element response.

It can be seen from Equation (23) that the inertial acceleration of fruit comes from vibration frequency v , response amplitude X and cross-vibration entrance angle θ' , which lays a theoretical foundation for the selection of experimental factors later.

5 Simulation analysis of Chinese wolfberry terminal branch model

Modal analysis is a method to study structural dynamics. Vibration mode is an inherent and integral characteristic of elastic structure, including the main vibration mode and modal response at the form's natural frequency and each order's natural frequencies. These parameters can be obtained by calculation, experiment, or finite element calculation. This paper will use this method to obtain its essential parameters.

5.1 Construction of physical model of Chinese wolfberry terminal branch based on measured data

To explore the mechanism of vibration fruit shedding, measuring the physical parameters and binding force of Chinese wolfberry branches and components is necessary. The main varieties of Chinese wolfberry in China are Ningqi No.1 and No.7. In this paper, Ningqi No.1, which is 4 years old, is selected as the primary test object.

The measuring method is as follows: measure the basic planting situation of Chinese wolfberry plants by means of a tape measure, ruler, vernier caliper, high-precision electronic scale and other tools, focusing on measuring the physical and mechanical parameters of Chinese wolfberry branches and components, including the length of Chinese wolfberry branches, the diameters of branches, the positions of mature fruits, immature fruits, olives, flowers, the average pitch of mature fruits, the average mass of mature fruits, the average binding force of mature fruits, the average mass of immature fruits, the average binding force of immature fruits, the average mass of olives, the average binding force of olives, the average mass of flowers, the average binding force of leaves, the average binding force of flowers, the average binding force of leaves, and the average binding force of immature fruits.

Through field investigation, the fruit-hanging length of Ningqi No.1 is between 500-600 mm, the third crop is the fruit-rich stage every year, and the number of flowers is basically zero, mainly composed of mature fruits, immature fruits, olives and leaves. The distribution of the physical parameters of each component is listed in Table 1, and the simplified physical parameters of the model are listed in Table 2.

As shown in Table 1, when considering physical modeling, the average pitch of mature fruit is 17mm, and the pitch of other fruits is 17 mm according to the characteristics of mature.

Combined with Table 1, the final branches of fruit-hanging Chinese wolfberry are simplified, and the relevant parameters are rounded. The adjusted data distribution is shown in the table below.

That is, the overall average pitch is 17 mm, the mature fruit-hanging segment is from 190 to 326 mm, and there are 9 nodes; each node bears 0.91 g of mature fruit; Immature fruit has 5 nodes from 326 to 394 mm, and the last 4 nodes have immature fruit, and the weight of each node is 0.56 g; Olive is from 394 mm to 547 mm, with 10 nodes, and the last 9 nodes are hung with olive, and the weight

of each node is 0.30 g. Finally, according to statistics, when the leaves are between 54-190 mm, there are 9 nodes, and the first 8 nodes are hung with leaves, so there are 30 nodes in total. If the leaves and other nodes are assigned values, the average leaf quality of each node is 0.12 g. The remaining 22 nodes increase the leaf mass, respectively. The adjusted model is listed in Table 3.

Table 1 Physical parameters of each component with measured branch length of 500-600 mm in the third crop for Ningqi No.1.

Branch number	Length/mm	Starting diameter/mm	End diameter/mm	Branch quality/g	Position of mature fruit at the beginning and end/mm	Position of immature fruit at the beginning and end/mm	Position of green fruit at the beginning and end/mm	Total mass of mature fruits/g	Total mass of immature fruits/g	Total mass of green fruits/g	Total mass of leaves/g	Average pitch of mature fruits/mm
1	590	3.23	1.03	3.95	280-400	400-465	465-470	7.15	1.82	2.35	4.01	14.38
2	560	3.06	1.26	3.86	150-260	240-380	380-560	11.25	2.61	1.84	3.8	13.86
3	550	3.37	1.18	4.15	230-420	420-480	480-550	7.48	1.26	2.3	3.77	19.5
4	560	3.38	1.05	3.68	210-380	380-410	410-560	7.41	2.4	2.44	3.76	14.55
5	560	3.33	1.06	4.88	147-315	315-380	380-560	11.64	1.61	3.26	3.98	15.11
6	510	3.0	1.1	2.64	130-240	250-330	310-510	6.90	3.31	4.46	2.98	17.5
7	510	2.6	1.0	2.08	160-250	265-350	280-510	5.62	2.71	2.40	3.06	23.75
Average	549	3.2	1.1	3.6	187-324	324-399	386-531	8.21	2.25	2.72	3.62	17

Table 2 Fruit and branch parameters of Ningqi No.1

Name	Mean	Standard deviation
Mature Chinese wolfberry quality m_1/g	0.69	0.16
Immature Chinese wolfberry quality m_2/g	0.30	0.24
Green fruit quality m_3/g	0.12	0.08
Flower quality m_4/g	/	/
Length of fruit-bearing branches L/mm	549	29.1
Diameter of the beginning of fruit-bearing branches d1/mm	3.2	0.29
Diameter of end of fruit-bearing branch d2/mm	1.1	0.09

Table 3 Simplified model of mass distribution of fruit-bearing branches

Name	Mean
Total length of branches L/mm	549
Total number of nodes N	30
Distribution range of nodes in branches /mm	54-547
Average quality of node distribution from 1 to 8 /g	0.12
Average quality of node distribution from 9 to 17 /g	1.03
Average quality of node distribution from 18 to 21 /g	0.68
Average quality of node distribution from 22 to 30 /g	0.42

5.2 Analysis of shedding conditions of components in Chinese wolfberry terminal branches

The binding force of each component was measured by a digital display push-pull meter (Shandu instrument, model SH-50, range 0-50 N, precision 0.01 N) or fruit hardness meter (model GY-4, range 0-4 N, precision 0.01 N). The picking time is July 3 -8, 2022. The mature fruit belongs to the third crop (the highest yield). All of them are in the picking period, and the mature fruits are eight to nine. Before the measurement, Ningqi No.1 plants distributed in different locations are measured by sampling method. Each Chinese wolfberry tree is taken as a sample, multiple groups of original data are detected by the above instruments, and the mean value processes the main targets. Statistics of the mechanical data of Chinese wolfberry terminal branches are listed in Table 4.

Assuming that the accelerations of mature Chinese wolfberry, immature Chinese wolfberry and olive are a_{t1} , a_{t2} and a_{t3} , respectively, the falling acceleration ranges of mature Chinese wolfberry, immature Chinese wolfberry and olive are shown in Equation (24).

$$\begin{cases} \frac{f_{1\min}}{m_1} \leq a_{t1} \leq \frac{f_{1\max}}{m_1} \\ \frac{f_{2\min}}{m_2} \leq a_{t2} \leq \frac{f_{2\max}}{m_2} \\ \frac{f_{3\min}}{m_3} \leq a_{t3} \leq \frac{f_{3\max}}{m_3} \end{cases} \quad (24)$$

According to the data in Table 3, the average mass of mature Chinese wolfberry (m_1) > immature Chinese wolfberry (m_2) > average mass of olive (m_3). By substituting the data in Table 3 and Table 4 into the above equation, the critical detachment acceleration range of mature fruit, immature fruit and olive can be obtained: $710 \text{ m/s}^2 \leq a_{t1} \leq 1290 \text{ m/s}^2$; $2400 \text{ m/s}^2 \leq a_{t2} \leq 4500 \text{ m/s}^2$; $7500 \text{ m/s}^2 \leq a_{t3} \leq 12 \text{ 000 m/s}^2$; Therefore, the reasonable acceleration to make mature Chinese wolfberry fall off but immature Chinese wolfberry and olive not fall off should satisfy $1290 \text{ m/s}^2 \leq a_t \leq 2400 \text{ m/s}^2$.

Table 4 Bounding force range

Name	Range
Binding force between mature Chinese wolfberry and fruit stalk f_1/N	0.49-0.89
Binding force between immature Chinese wolfberry and fruit stalk f_2/N	0.72-1.35
Binding force between olive and fruit stalk f_3/N	0.9-1.44
The binding force between flowers and flower stalks f_4/N	/

5.3 Modal analysis

A modal analysis of Chinese wolfberry fruit-hanging branches was carried out with Workbench 2022R1 software from ANSYS products 2022R1. To be consistent with the theoretical model of the forced vibration picking model of the fruit-hanging branches of Chinese wolfberry, it was planned to analyze the modal, forced vibration displacement and acceleration response of the fruit-hanging branches as a whole. According to Tables 2 and 3, the fruit-hanging areas' third fruit-hanging branches of Chinese wolfberry are divided into four sections. The leaf mass is equally equivalent along the branches. In contrast, the total weight of mature Chinese wolfberry is evenly distributed in the second section of the branches (the beginning and end position of mature fruits). The total mass of immature fruit is evenly distributed in the third branch (the beginning and end position of immature fruit), and the total mass of green fruit is evenly distributed in the fourth branch (the beginning and end position of green fruit). A simplified model of the third

crop of Chinese wolfberry in summer fruits is constructed, and the preliminary modeling by Solidworks software is shown in Figure 4.

Import the model into the finite element software ANSYS Workbench 2022R1, add material properties to its engineering data, refer to the related literature^[21], and combine with the small



Figure 4 Simplified model of terminal branch for Chinese wolfberry

The model is divided into grids, with 51 245 nodes and 27 563 units. The large-diameter end of the cantilever beam is constrained, and the maximum modal order is set to 10 orders in modal analysis. Finally, the first 10 natural frequencies of the fruit-hanging branches are obtained by solving them, and the arrangement is listed in Table 5.

Table 5 First 10 natural frequencies of Chinese wolfberry branches for Ningqi No.1

Order	1	2	3	4	5	6	7	8	9	10
Natural frequency/ Hz	0.996	1.003	5.343	5.365	13.863	13.924	25.698	25.784	38.419	41.243

The above table provides a basis for this paper to study the amplitude amplification of each component of the corresponding branch when the forced vibration frequency approaches the corresponding natural frequency. Because of its approximate symmetrical cone, the natural frequencies of every two orders are closely distributed. See the following harmonic response analysis for details of obtaining ideal picking parameters.

5.4 Harmonic response analysis

Add the harmonic response analysis module based on Modal analysis module 4.1.3. In this research, the amplitude is fixed, and the maximum amplitude response value of each branch position is studied by frequency sweeping. The preset amplitude is 15 mm, which is applied to the distance between the adjacent first ripe fruit of 17 mm, that is, from the large-diameter end face as the coordinate origin and 183 mm in the Z-axis direction, and the displacement response of each branch position under each frequency condition is solved by using the complete analytical method of harmonic response analysis. The relationship between

mechanical parameters of the actual branches, appropriately lower the axial elastic modulus of branches, and the parameters of fruit-hanging branches were set as follows: density 1008 kg/m³, $E_x=23.43$ MPa, $E_y=23.43$ MPa, $E_z=270$ MPa, $u_{xy}=0.3$, $u_{yz}=0.15$, $u_{xz}=0.15$, $G_{xy}=40.12$ MPa, $G_{yz}=4.02$ MPa, $G_{xz}=4.02$ MPa.

natural frequencies and high-quality fruit removal is studied to select the ideal operating frequency.

As can be seen from Figure 5, the excitation position is located at 183 mm along the Z-axis in the fully constrained position, and there are two equilibrium points on the branch with a total length of 549 mm. The displacement and acceleration responses from the excitation position to the root of the branch gradually decrease, and the displacement and acceleration responses from the excitation position to the tip of the branch fluctuate, increasing, decreasing and then increasing, and the maximum position of total deformation is the tip. As can be seen from Figure 5a, the operating frequency is 13 Hz, which is close to the natural frequency of the 5th or 6th order, and the critical fruit shedding requirement cannot be achieved by measuring the fruit abscission acceleration in the mature area. However, the natural frequency of the 9th order reaches 38.419 Hz. In view of the previous related research^[9], this frequency requires higher quality and structure of working parts, so it needs to be studied. This paper focuses on the response analysis of the natural frequency approaching the 7th or 8th order. As can be seen from Figure 5c, when the operating frequency is 24 Hz, both the mature and semi-mature fruit areas meet the requirements of fruit peeling, while the terminal amplitude is 109.85 mm, and the magnification is 7.32 times. Assuming that $\theta=90^\circ$, $\cos vt=1$, $l=0.015$ m, the theoretical maximum acceleration is 18 293.26 m/s², exceeding. Therefore, the response values of each node of the branch at frequencies of 23 Hz and 24 Hz are extracted, and at the same time, the response accelerations of 30 nodes are extracted. Combined with Equation (23), the maximum acceleration of the fruit corresponding to the displacement of each node is calculated, and two decimal places are reserved, arranged as follows.

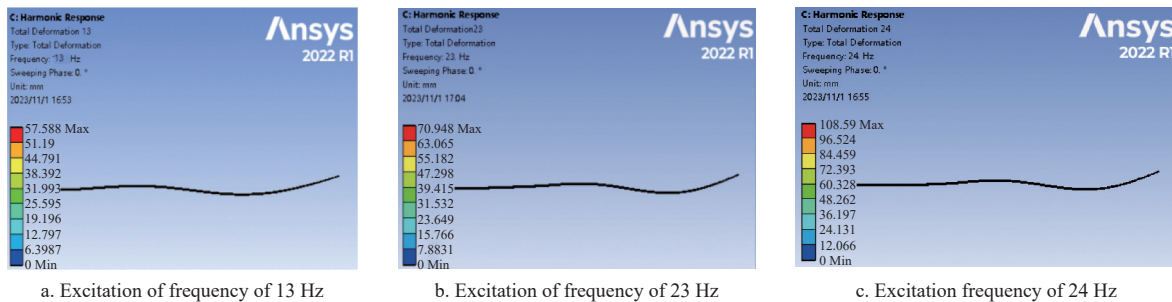


Figure 5 Cloud map of displacement response of Chinese wolfberry branches under excitation of different frequencies with a displacement of 15 mm

As can be seen from Table 6 and Figure 6, when the length of the fruit stalk is fixed, the acceleration of the fruit increases with the amplitude of the branch response (the order is greater than 1), so the acceleration of the fruit is greater than the acceleration of the branch

node; When the response displacement is lower than the forced vibration amplitude of the branch, the acceleration of the fruit decreases with the decrease of the response amplitude (the order is between 0 and 1). Hence the acceleration of the fruit is less than the

response acceleration of the branch node. At the same time, the closer to the natural frequency, the higher the acceleration value of the branches, and the greater the influence of acceleration on the fruits. When the frequency is 24 Hz, the fruit accelerations between nodes 10-16 are all greater than 710 m/s², and those between nodes 10-15 are all greater than 1000 m/s². When the excitation point is the eighth node, the effective picking interval can start from the excitation position, which is 34-136 mm away from the excitation position respectively. The ripe fruits in this interval can be peeled off with high probability, and the effective picking interval is identified as 102 mm. In addition, the two terminal nodes have reached the condition of green fruit detachment, but their fruit detachment is greatly affected by the terminal mass components. The relationship between terminal misreading and test parameters will be discussed through experiments later.

Table 6 Calculation of node response and node fruit acceleration

Node	23 Hz			24 Hz		
	Simulated maximum displacement /mm	Simulated maximum acceleration /m·s ⁻²	The maximum acceleration calculation of node fruits /m·s ⁻²	Simulated maximum displacement /mm	Simulated maximum acceleration /m·s ⁻²	The maximum acceleration calculation of node fruits /m·s ⁻²
1	3.38	65.57	15.91	1.58	37.53	3.78
2	5.16	102.56	37.07	2.67	61.21	10.81
3	6.98	143.53	67.83	3.91	88.72	23.18
4	8.68	180.69	104.90	5.30	121.37	42.58
5	10.24	211.36	145.99	6.96	159.35	73.44
6	11.71	238.58	190.91	9.02	205.63	123.34
7	13.22	273.35	243.32	11.60	264.60	203.99
8	15.00	313.26	313.26	15.00	341.09	341.09
9	17.89	372.82	445.60	20.31	463.62	625.33
10	21.12	439.97	621.03	26.66	606.67	1077.49
11	23.85	497.74	791.96	32.40	738.59	1591.41
12	25.31	528.41	891.88	36.48	829.68	2017.44
13	25.02	522.41	871.56	37.74	858.21	2159.21
14	22.69	468.73	716.79	35.70	812.14	1932.09
15	18.37	385.18	469.83	30.35	690.06	1396.40
16	12.34	257.73	212.01	21.91	496.15	727.74
17	5.16	105.53	37.07	11.32	254.99	194.26
18	2.70	50.356	10.15	1.64	37.28	4.08
19	9.95	209.99	137.84	12.77	289.29	209.61
20	16.30	341.44	369.91	23.13	528.31	811.04
21	20.98	438.41	612.82	31.27	712.08	1482.34
22	23.22	484.96	750.67	35.66	811.83	1927.76
23	22.38	467.45	697.34	35.27	801.08	1885.83
24	18.06	375.37	454.11	29.23	664.74	1295.24
25	10.11	211.06	142.31	17.54	394.01	466.39
26	1.61	36.656	3.61	1.64	35.58	4.08
27	15.29	323.32	325.49	22.16	501.76	744.44
28	31.48	652.00	1379.73	47.42	1083.50	3408.90
29	49.61	1039.5	3426.59	75.98	1734.70	8751.64
30	68.74	1438.9	6578.75	106.27	2426.70	17120.34

In a word, when the natural frequency is close to the 7th order of 24 Hz, the amplitude is 15 mm, and the exciting position is 34mm away from the fruit to be picked. The picking interval of mature Chinese wolfberry can reach 102 mm, which meets the requirement of picking only the ripe fruit and not picking other fruits by mistake, which lays a theoretical foundation for the following experiments.

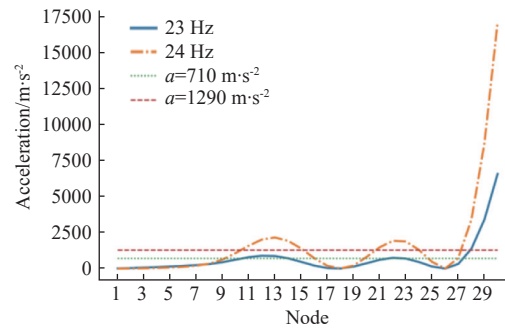
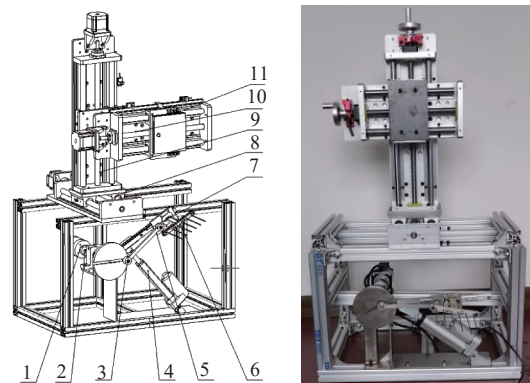


Figure 6 The maximum acceleration calculation of node fruits

6 Design of multi-parameter adjustable test-bed for reciprocating vibration picking

6.1 Structural design of test bench

According to the four-level data requirements of vibration frequency, amplitude and cross-vibration entrance angle, the test-bed is designed as shown in Figure 7.



1. Servo drive motor; 2. Coupling; 3. Crank length adjustment mechanism;
4. Electric push rod control system; 5. Connecting rod; 6. Fork rod;
7. Reciprocating motion slider; 8. Front and rear position adjustment mechanism;
9. Up and down position adjustment mechanism; 10. Left and right position adjustment mechanism; 11. Branch clamping mechanism

Figure 7 Design and trial production of reciprocating vibration picking multi-parameter adjustable test bench

As shown in Figure 7, to ensure the forced movement effect of reciprocating branches, spring steel is selected as the fork bar material, the diameter of elastic teeth is 2 mm, and the length of the fork bar is 8cm, which is light and ensures rigidity. To ensure four groups of gaps, four groups of U-shaped fork bars with different gaps are trial-produced through mold opening and special heat treatment. At the same time, to facilitate disassembly, the hinge handle of the fork bar is designed with nylon material and hinged with four groups of bolts. The angle rotation adjustment mechanism of the crank-slider mechanism is created by using an electric push rod, and the hinged dial of the intermediate coupling disc accurately adjusts the vibration angle. By adjusting one end of the connecting rod of the crank slider to be hinged at the diameter position of the disc, the reciprocating stroke adjustment is realized, that is, the amplitude control is realized; Finally, according to the selected servo motor, it is connected to the computer through the interface, and the frequency of the driving motor is accurately controlled through the parameter input window of the frequency control interface.

6.2 Reciprocating motion analysis

The device adopts a servo motor as a power source, and its

vibration model is simplified as a crank-slider mechanism without eccentricity, which is transformed into linear reciprocating motion^[22] through uniform crank rotation to drive the vibrating fork to realize reciprocating motion. As shown in Figure 8. Its motion characteristics are as follows:

$$\begin{cases} x = X_0 \cos \gamma + \sqrt{L^2 - X_0^2 \sin^2 \gamma} \\ \gamma = vt \end{cases} \quad (25)$$

where, X_0 is the crank length, m. L' is the length of connecting rod, m. γ is the crank rotation angle, rad.

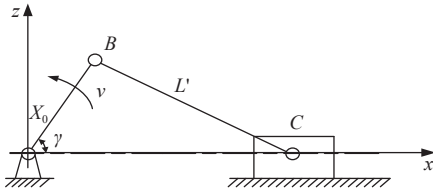


Figure 8 Motion model of crank-slider mechanism

Then the motion acceleration equation:

$$x'' = -X_0 v^2 \left[\cos \gamma + \frac{X_0 \cos 2\gamma}{(L^2 - X_0^2 \sin^2 \gamma)^{\frac{1}{2}}} + \frac{X_0^3 \sin^2 2\gamma}{4(L^2 - X_0^2 \sin^2 \gamma)^{\frac{3}{2}}} \right] \quad (26)$$

According to the law of motion, it can be obtained that $\gamma = 0$ and the maximum acceleration is:

$$a_{z0} = -X_0 v^2 \left(1 + \frac{X_0}{L'} \right) \quad (27)$$

According to the binding force between the fruit quality and the fruit stalk, it can be seen that the acceleration of Chinese wolfberry is shown in Equation (24), and it is found that the vibration acceleration alone cannot force Chinese wolfberry to shed fruit. Therefore, this study establishes the theoretical basis for the change law of acceleration amplification coefficient of the target fruit through the differential equation of branch vibration and the infinitesimal motion model of fruit-hanging branches.

Because of $X_0 \ll L$, $a_{z0} = -X_0 v^2$, combined with the above experimental conclusions: the reasonable acceleration a_t of immature Chinese wolfberry and olive should satisfy $1290 \text{ m/s}^2 \leq a_t \leq 2400 \text{ m/s}^2$ (See the following test). The amplitude range is 13-19 mm, the rotation speed range is 1100-1400 r/min, and the frequency range is 18.33-23.22 Hz. According to the $1290 \text{ m/s}^2 \leq |a_t| = |\ddot{\theta}^2| = \beta X_0 v^2 \leq 2400 \text{ m/s}^2$ relation, it can be seen that the maximum input acceleration is 172-408 m/s^2 , and the response acceleration on the branches is greater than 1290 m/s^2 , and the magnification β is 3.2-7.5. The following will study the optimal combination relationship of key operation parameters through specific tests.

7 Experimental design and result analysis

7.1 Experimental design

On July 6th, 2022, the National Chinese wolfberry Engineering Technology Research Center was in charge of the experimental base of Chinese wolfberry cultivation and plantation forest farm. Ningqi No.1, which was 4 years old, was taken as the research object, and related experiments were carried out based on the trial-production test bench.

Based on the conclusion of simulation operation parameters in the fourth section and the analysis of the vibration harvesting effect of Chinese wolfberry branches in the early stage^[11], vibration frequency and amplitude are significant factors leading to the

separation of Chinese wolfberry, so the motor driving speed is 1100=1400 r/min, that is, 18.3-23.3 Hz and the amplitude is 13-19 mm; According to the infinitesimal model of inertia force between branches and fruits, the cutting angle of cross vibration has an influence on the fruit shedding of Chinese wolfberry, and the entrance angle is from 45° to 90°. According to the selected amplitude, it is convenient for forks to enter branches, the gap between forks is 13 mm, and six forks are equally distributed. Therefore, taking frequency, amplitude and entrance angle as test factors, in order to verify the accuracy of the design of each parameter combination, it is planned to carry out three-factor and four-level orthogonal tests on the selected three test factors, and adopt $L_{16}(4^3)$ orthogonal test method^[22]. The designed three-factor four-level test table is listed in Table 7.

Table 7 Design of experimental factors and levels for high quality picking of Chinese wolfberry

Level	Index		
	Vibration frequency (A) /Hz	Amplitude (B)/mm	Entrance angle (C)/(°)
1	18.3	13	90
2	20.0	15	75
3	21.7	17	60
4	23.3	19	45

Taking net picking rate, damage rate and false picking rate as test indexes, the influence law and optimal combination of three influencing factors on the three indexes are obtained. The net picking rate refers to the percentage of the total number of ripe Chinese wolfberry picked in a certain picking interval to the total number of ripe fruits in the interval^[23], and the calculation equation of the net picking rate of Chinese wolfberry is:

$$p_c = \frac{S_c}{S_z} \times 100\% \quad (28)$$

where, p_c is net picking rate, %; S_c is total number of mature Chinese wolfberry picked in a certain condition; S_z is total number of mature Chinese wolfberry to be picked in a certain picking interval.

Damage rate refers to the proportion of damaged Chinese wolfberry. Because fresh fruit damage is not easy to find, dried Chinese wolfberry was processed in this experiment, and Chinese wolfberry identification experts were asked to make statistics on the damage caused by mechanical action. The calculation equation of the damage rate is as follows:

$$p_s = \frac{S_s}{S_c} \times 100\% \quad (29)$$

where, p_s is damage rate, %; S_s is total number of damaged fruits.

The false picking rate refers to the ratio of the total number of picked immature Chinese wolfberry to the total number of picked mature and immature Chinese wolfberry, and the calculation equation of the false picking rate is:

$$p_w = \frac{S_w}{S_c + S_w} \times 100\% \quad (30)$$

where, p_w is false picking rate, %; S_w is total number of immature Chinese wolfberry picked under certain conditions.

7.2 Test conditions and result analysis

7.2.1 Test conditions

As shown in Figure 9, the picking experiment was carried out in the experimental base. Taking the manual operation of one branch as the standard, the test conditions were unified. The vibration-picking device vibrated one branch at a time, and the

operation time was 3 s. In addition, the selection conditions of the operation position: in view of the above simulation conclusion, the excitation point is about 34 mm on the upper branch of the first ripe fruit, and the interval to be picked is 100 mm. If the actual interval to be picked is more significant than 100 mm, Moreover, it is convenient for the test, and the clamping mechanism is replaced manually, and it is lifted to the ideal position to assist the test; According to the orthogonal test table, the batch test was carried out by using the multi-parameter adjustable picking test bench, and the statistical test results are listed in Table 8.



Figure 9 Test site of multi-parameter control test bench

Table 8 Test and results on the fruit detachment of Chinese wolfberry

Test No.	Index			Performance parameters			
	A	B	C	Rate of picking (p_c)/%	Damage rate (p_s)/%	Rate of error picking (p_w)/%	Comprehensive score (z_p)/%
1	1	1	1	74.51	2.63	0	86.60
2	1	2	2	81.52	0	0	90.76
3	1	3	3	95.59	4.62	8.11*	94.61
4	1	4	4	99.56	7.43	12.72*	94.74
5	2	1	2	89.80	3.79	0	93.95
6	2	2	1	98.82	0	0	99.66
7	2	3	4	97.22	5.71	8.86*	94.97
8	2	4	3	99	5.9	12.1*	95.00
9	3	1	3	89.89	1.12	0	94.67
10	3	2	4	100	0	3.76	99.06
11	3	3	1	94.59	1.43	8.64	94.78
12	3	4	2	100	5.98	12.68	95.34
13	4	1	4	94.44	1.47	0	96.85
14	4	2	3	100	0	8.56*	97.87
15	4	3	2	97.35	2.73	9.60*	95.67
16	4	4	1	100	3.75	13.23*	95.76

Note: * means that the data contains the false picking of green fruits at the tip vibration end of branches.

7.2.2 Experimental results and analysis

According to the experimental results, the optimal level, primary and secondary order and optimal combination of factors affecting the net picking, damage and false picking rate are obtained. The structural optimization of the reciprocating vibration picking device and the optimal operation parameter configuration test are multi-index orthogonal tests. Therefore, the comprehensive scoring method is adopted to convert the test results of the three indexes into a unified, comprehensive index. According to the importance of the index, the weights of the net picking rate, damage rate and false picking rate are set^[24], and the weights of the three

indexes are set to 0.5, 0.25 and 0.25 respectively, according to the requirements of experts on picking standards of Chinese wolfberry. The greater the weighted average, the better the picking effect. Before calculating the weighted average, make the following changes to the scoring calculation equation.

$$z_p = 0.5p_c + 0.25p_{sp} + 0.25p_{wp} \quad (31)$$

where, $p_{sp} = 1 - p_s$, $p_{wp} = 1 - p_w$, p_{sp} is damage rate score value, %; p_{wp} is rate of error picking, %; z_p is comprehensive score value, %.

Therefore, the comprehensive score can be calculated according to the test results listed in Table 8, and the range analysis of the orthogonal test results is listed in Table 9.

Table 9 Range analysis of orthogonal experiment results

Test indicators		A	B	C
Rate of picking	T_1	87.80	87.16	91.98
	T_2	96.21	95.09	92.17
	T_3	96.12	96.19	96.12
	T_4	97.95	99.64	97.81
	Extreme difference R	10.15	12.48	5.83
Damage rate	T_1	3.67	2.25	1.95
	T_2	3.85	0	3.13
	T_3	2.13	3.62	2.91
	T_4	1.99	5.77	3.65
	Extreme difference R	1.86	5.77	1.70
Rate of error picking	T_1	5.21	0	5.47
	T_2	5.24	3.08	5.57
	T_3	6.27	8.80	7.19
	T_4	7.85	12.68	6.34
	Extreme difference R	2.64	12.68	1.72
Comprehensive score	T_1	91.68	93.02	94.20
	T_2	95.90	96.84	93.93
	T_3	95.96	95.01	95.54
	T_4	96.54	95.21	96.41
	Extreme difference R	4.86	3.82	2.48
Optimal level		$A_4B_2C_4$		
Primary and secondary order		$A > B > C$		

Table 9 shows that the greater the range of each factor, the greater its influence on the test index. The primary and secondary relationship of the influencing factors of net picking rate, damage rate, false picking rate and the comprehensive score is determined through the range. Among them, taking the net picking rate as the experimental index, the primary and secondary relations of the factors affecting the picking rate are amplitude, frequency and entrance angle, and the increase of amplitude is more beneficial to the fruit removal of Chinese wolfberry; Taking the damage rate as the test index, the primary and secondary relations of the factors affecting the damage rate are amplitude, frequency and entrance angle, and the more the amplitude increases, the more likely it is to cause damage to Chinese wolfberry. Taking the false picking rate as the test index, the primary and secondary factors affecting the false picking rate are amplitude, frequency and entrance angle. The greater the amplitude, the greater the inertia force and the entrance angle has little influence on the false picking of immature and green fruits. In addition, with the increase of frequency and amplitude, the false picking rate increases significantly, and the sharp increase of data is mainly due to the vibration of the tip, which is consistent with the response acceleration of the simulated branch tip. Excessive response force destroys the branch with poor stiffness at

the end of the branch and causes a fracture. With the synchronous reduction of frequency and amplitude, the net picking rate drops sharply, and the false picking rate drops significantly. As shown in Table 8, the false-picking rate of several data groups drops to zero. Therefore, under the premise of ensuring the picking quality, the amplitude and frequency of operation should be reduced as much as possible.

In addition, through comprehensive evaluation, it is determined that the primary and secondary relationship of each factor is $A > B > C$, that is, frequency, amplitude and entrance angle, and the optimal combination is $A_4B_2C_4$, that is, the vibration frequency is 23.3 Hz, the amplitude is 15 mm and the entrance angle is 45° . However, according to Table 7, the frequency is 20 Hz or 23.3 Hz, and the comprehensive score of picking Chinese wolfberry is close. The high-frequency operation will cause vibration and noise pollution of the reciprocating vibration mechanism and reduce the comfort of workers. Therefore, the frequency is set to 20 Hz, and the optimal combination is changed to $A_2B_2C_4$.

According to the optimal operation parameters, the vibration frequency is 20 Hz, and the amplitude is 15 mm; the hand-held vibration picking device is guided to trial-produce, and the above picking conditions are repeated. After a large number of experiments, the site is shown in Figure 10. According to statistics, the net picking rate of Chinese wolfberry is 96.13%, the damage rate is 1.13%, and the false picking rate is 3.23%, which meets the high-quality requirements of farmers for mechanized Chinese wolfberry harvesting.



Figure 10 Experiment of hand-held Chinese wolfberry vibrating device

7.3 Picking efficiency test

A comparative experiment on picking efficiency was carried out to verify the working effect of the hand-held Chinese wolfberry vibrating picking device under this combination and test its advantages compared with manual work. Select the quality of ripe fruits picked in unit time. In order to compare and analyze the efficiency of mechanical picking and manual picking, a manual picking experiment was carried out, and five skilled workers were selected to pick the fruit in the ideal Chinese wolfberry garden for 10 min. Subsequently, the hand-held vibration picking device test was carried out, and the picking operation parameters were adjusted with frequency of 20 Hz, amplitude of 15 mm, and fork vibration entrance angle. The picking test was still carried out on the fruit-hanging Chinese wolfberry branches of Ningqi No.1, which were 4 years old. Soft fruit-hanging materials were laid on the ground, and artificial auxiliary collection was carried out. Five tests were counted, each lasting for 10 min. Table 10 lists the data after the test. The results show that the efficiency of mechanized picking is 30.28 kg/h, which is 6.65 times that of manual picking.

Table 10 Comparative experiment of picking efficiency

Parameter	Numerical value
Average manual picking efficiency/kg·h ⁻¹	4.55
Average picking efficiency of the machine/kg·h ⁻¹	30.28
Ratio of machine to human picking efficiency	6.65

8 Conclusions

(1) In this paper, a simplified cantilever beam forced vibration picking model and fruit-hanging micro-element branch motion model are constructed by analyzing the principle of forced vibration of fruit-hanging branches of Chinese wolfberry. The solution method of inertial force excited by forced vibration of branches to the fruit terminal is obtained. The theoretical parameters affecting fruit separation are frequency, amplitude, and entrance angle.

(2) Combined with the forced vibration model of the cantilever beam, the typical fruit-hanging branch of the third crop of Chinese wolfberry in summer fruits is modeled by finite element software, and the modal harmonious response is analyzed. The results show that the natural frequency is close to the seventh order, and the fruit shedding effect is remarkable, and when the amplitude is 15 mm and the frequency is 24 Hz, the fruit falling interval can reach 102 mm. The response of displacement and acceleration from the excitation position to the root of the branch decreases gradually, and the displacement and acceleration responses from the excitation position to the tip of the branch show the fluctuation law of increasing and decreasing, increasing and decreasing, and then increasing, meanwhile, the mature fruits of fruit falling interval are beneficial to shedding, so the forced vibration position is preferentially applied to the upper branch position of the mature fruits.

(3) Based on the built test-bed with adjustable parameters of frequency, amplitude, and entrance angle, a three-factor and four-level orthogonal experiment and a comprehensive evaluation model of high-quality picking are designed to test the third crop of fruit-hanging branches of Chinese wolfberry in summer fruits for Ningqi No.1. The results show that the primary and secondary relations of the factors affecting the picking effect are frequency, amplitude and entrance angle in turn, and the best combination of operations is a frequency of 20 Hz, amplitude of 15 mm and an entrance angle, which guides the trial to formulate a handheld vibration picker, and the results show that the net picking rate of Chinese wolfberry is 96.13%, the damage rate is 1.13%, the false picking rate is 3.23%, and the mechanized picking efficiency is 30.28 kg/h, which is 6.65 times that of manual picking, meeting the requirements of farmers for high efficiency and high quality of Chinese wolfberry harvesting.

(4) This paper reveals the fruit shedding mechanism of fruit-hanging branches in the third crop of Ningqi No.1 in summer fruits. In the later period, we can use this research method to deeply study the multi-parameter optimization of fruit-hanging branches in different varieties of summer fruits and autumn fruits and obtain the optimal operation parameter configuration decision under multiple conditions to guide the reciprocating vibration harvesting device or equipment for efficient and high-quality picking.

Acknowledgements

The research work was financially supported by the National natural science foundation of China (Grant No. 32201681), Key Research and Development Projects in Ningxia Hui Autonomous Region (Grant No. 2021BEF02001), Subject of Independent

Innovation Fund for Agricultural Science and Technology in Ningxia Hui Autonomous Region (Grant No. NGSB-2021-2-05) and Demonstration and popularization of equipment and technology in modern agricultural machinery, Jiangsu Province (Grant No. NJ2021-18).

[References]

- [1] Amagase H, Farnsworth N R. A review of botanical characteristics, phytochemistry, clinical relevance in efficacy and safety of *Lycium barbarum* fruit (Goji). *Food research international*, 2011; 44(7): 1702–1717.
- [2] Ma J W. Research status and prospect of the mechanized technology of picking wolfberry in China. *Mechanical Research & Application*, 2017; 30(4): 151–153. (in Chinese)
- [3] Cao L, Zhang A L. Study on present situation development stages and trends of Chinese wolfberry industry. *Forest Resources Management*, 2015; 2: 4–8, 30. (in Chinese)
- [4] Li Q, Ye L Q, An W. The suitable working of wolfberry harvest machine. *Journal of Agricultural Mechanization Research*, 2009; 6: 126–128. (in Chinese)
- [5] Shi Z G, Xiao H R, Wan R, Zhang Z, Wang Y J, Mei S, et al. Research progress of Chinese wolfberry picking machine. *Agricultural Science & Technology and Equipment*, 2016; 263(5): 53–56. (in Chinese)
- [6] Li C, Xing J J, Xu L M, He S L, Li S J. Design and experiment of wine grape threshing mechanism with flexible combing striping monomer. *Transactions of the CSAE*, 2015; 31(6): 290–296. (in Chinese)
- [7] Ye L Q, Li Q, Chen J Y, An W. Study on picking performance of portable wolfberry picker. *Ningxia Journal of Agriculture and Forestry Science and Technology*, 2009; 4: 4–5, 56. (in Chinese)
- [8] Zhao Y, Xiao H R, Wang X J, Shi Z G, Mei S, Ding W Q. Design and fruit drop experiment of 4GQB-3300 *Lycium* L. harvester based on standardized planting mode. *Journal of Chinese Agricultural Mechanization*, 2019; 40(6): 43–51. (in Chinese)
- [9] Li C S, Gao Z J, Kan Z, Wang L H, Yuan P P, Wang Z. Experiment of fruit-pedicle vibration separation of wine grape. *Transactions of the CSAE*, 2015; 31(9): 39–44. (in Chinese)
- [10] Wang C Q, Xu L Y, Zhou H P, Cui Y M, Cui H. Development and experiment of eccentric-type vibratory harvester for forest-fruits. *Transactions of the CSAE*, 2012; 28(16): 10–16. (in Chinese)
- [11] Song Z Y, Mei S, Xiao H R, Shi Z G, Wang J P, Zhao Y, et al. Comparative test and analysis on the harvesting methods of Chinese wolfberry fruit. *Journal of Chinese Agricultural Mechanization*, 2019; 40(10): 110–116. (in Chinese)
- [12] Wang J P, Mei S, Xiao H R, Zhao Y, Zhou H P. Research on mechanized harvesting methods of Chinese wolfberry Fruit. *IFAC-PapersOnLine*, 2018; 51(17): 223–226.
- [13] Zhang Z, Xiao H R, Ding W Q, Mei S. Mechanism simulation analysis and prototype experiment of Chinese wolfberry harvest by vibration mode. *Transaction of the CSAE*, 2015; 31(10): 20–28. (in Chinese)
- [14] Xu L M, Chen J W, Wu G, Yuan Q C, Ma S, Yu C C, et al. Design and operating parameter optimization of comb brush vibratory harvesting device for wolfberry. *Transactions of the CSAE*, 2018; 34(9): 75–82. (in Chinese)
- [15] Hu M M, Wan F X, Du X L, Huang X P. Design of vibrating wolfberry picking machine. *Journal of Chinese Agricultural Mechanization*, 2018; 39(7): 25–29. (in Chinese)
- [16] Mei S, Xiao H R, Shi Z G, Jiang Q H, Zhao Y, Ding W Q. Design and test of low-loss *Lycium barbarum* harvesting technology and equipment based on reciprocating vibration method. *Journal of Chinese Agricultural Mechanization*, 2019; 40(11): 100–105, 208. (in Chinese)
- [17] Zhang Z. The design and experiment of *Lycium barbarum* harvesting mechanism by vibration mode. Nanjing: Nanjing Research Institute for Agricultural Mechanization, Ministry of Agriculture Affairs, 2016. (in Chinese)
- [18] Zhang Y M. Mechanical vibrations (Second edition). Beijing: Tsinghua University Press, 2017. (in Chinese)
- [19] Bao Y D. Research on vibration characteristics and numerical simulation of blueberry mechanization harvesting. Northeast Forestry University, 2015. (in Chinese)
- [20] Cooke J R, Rand R H. Vibratory fruit harvesting: A non-linear fruit-stem dynamics. *J Agric Engng Res*, 1970; 15(4): 347–363.
- [21] Zhao J. Key technologies of vibrating and comb brushing harvesting for *Lycium barbarum* L. Northwest A&F University, 2022. (in Chinese)
- [22] Peng Y, Zhang Z Y, Liu Y, Xu T S, Wang R J. Design and experiment of accurate clamping vibration wolfberry harvesting machine. *Mechanical Research & Application*, 2018; 31(6): 123–129, 132. (in Chinese)
- [23] Zhang W Q, Zhang M M, Zhang J X, Li W. Design and experiment of vibrating wolfberry harvester. *Transactions of the CSAM*, 2018; 49(7): 97–102. (in Chinese)
- [24] Zhang W Q, Li Z Z, Tan Y Z, Li W. Optimal design and experiment on variable pacing combing brush picking device for Chinese wolfberry. *Transactions of the CSAM*, 2018; 49(8): 83–90. (in Chinese)